THE EFFICIENCY OF TAPERED STEEL SECTION WITH PERFORATION UNDER SHEAR BUCKLING BEHAVIOUR

LOCK PUI YEE

SCHOOL OF CIVIL ENGINEERING
UNIVERSITI SAINS MALAYSIA
2018

BLANK PAGE

THE EFFICIENCY OF TAPERED STEEL SECTION WITH PERFORATION UNDER SHEAR BUCKLING BEHAVIOUR

By

LOCK PUI YEE

This dissertation is submitted to

UNIVERSITI SAINS MALAYSIA

As partial fulfilment of requirement for the degree of

BACHELOR OF ENGINEERING (HONS.)
(CIVIL ENGINEERING)

School of Civil Engineering,
Universiti Sains Malaysia

June 2018

SCHOOL OF CIVIL ENGINEERING
ACADEMIC SESSION 2017/2018

FINAL YEAR PROJECT EAA492/6
DISSERTATION ENDORSEMENT FORM

Title: THE EFFICIENCY OF TAPERED STEEL SECTION WITH PERFORATION UNDER SHEAR BUCKLING BEHAVIOUR

Name of Student: LOCK PUI YEE

I hereby declare that all corrections and comments made by the supervisor(s) and examiner have been taken into consideration and rectified accordingly.

Signature: Approved by:

_____ _____

(Signature of Supervisor)

Date : Name of Supervisor :

Date :

Approved by:

_____

(Signature of Examiner)

Name of Examiner :

Date :

ACKNOWLEDGEMENT

First and foremost, I would like to thank Universiti Sains Malaysia for giving me this opportunity to complete my final year project dissertation. I would also like to express my full gratitude to my supervisor, Associate Professor Dr Fatimah De'nan. Throughout this final year, she has been guiding and sharing me the knowledge and suggestions to produce a good quality project. Without her, I can hardly produce my result and complete my dissertation on time.

Next, my sincere and special thanks to Ling Jin Ying, who is a postgraduate student from USM for helping and shearing me with the correct simulation method in my nonlinear analysis study.

I would also like to thank my friends for supporting me and encouraging me to produce a better quality of dissertation.

ABSTRAK

Untuk mencapai pengoptimuman dalam pembinaan, konventional rasuk I telah digantikan oleh keratan tirus dengan perbukaan. Idea pembukaan and tirus pada profil web adalah disebabkan oleh *moment gradient* yang tidak seragam sepanjang rasuk dalam kebanyakkan kes. Bentuk keratan rentas harus berubah secara linear dengan *moment gradient* untuk mencapai efisien yang lebih tinggi dengan kos yang lebih rendah. Pengagihan semula tegasan dari beban adalah disebabkan oleh ketirusan dan pembukaan pada profil web. Oleh itu, analisis unsur terhingga secara tidak linear telah dijalankan untuk menyiasat corak ubah bentuk ricih dan efisien bahagian keluli tirus dengan bukaan dalam kajian ini. Sebanyak 148 model telah disimulasi melalui perisian LUSAS dengan parameter pembolehubah yang ditetapkan seperti nisbah penirusan, bentuk pembukaan, saiz pembukaan dan susun atur pembukaan. Keluli tirus dengan pembukaan mempunyai kritikal beban ricih dan efisien yang lebih rendah berbanding dengan keluli tirus tanpa pembukaan, tetapi ia memperoleh kritikal beban ricih dan efisien yang lebih tinggi berbanding dengan keratan seragam tanpa pembukaan. Saiz pembukan yang kecil dengan penirusan nisbah yang rendah menyumbang kepada kapasiti ricih dan efisient yang lebih besar. Perbezaan dalam susun dan jarak pembukaan akan mempengaruhi kekuatan ricih dan efisien keluli tirus dengan pembukaan. Model yang mempunyai efisien tertinggi adalah keratan yang mempunyai pembukaan bentuk berlian dengan 0.4D saiz dengan 0.3 nisbah penirusan. Beban ricih kritikal dan efisien masing-masing telah dikurangkan sebanyak 14.39% dan 13.91% apabila pembukaan ditambah pada keluli tirus. Sebanyak 0.56% bahan keluli boleh dijimatkan dalam pembinaan yang sama dengan keluli tirus yang mempunyai pembukaan berbanding dengan keluli tirus tanpa pembukaan.

ABSTRACT

For optimization in construction, conventional I-beam is widely replaced by tapered and perforated section. The ideas of tapering and perforating the web of the section comes from the reason of ununiform moment gradient throughout the beam for most cases. The cross-sectional shape of beam is varied linearly to the moment gradient to achieve target of higher efficiency with lower cost. The redistribution of the stress from the applied load is caused by the tapering and perforating on the web profile. Hence, a non-linear finite element analysis was conducted to investigate the shear deformation pattern and efficiency of the tapered steel section with perforation in this research. A total of 148 models were simulated via LUSAS software with the variables parameters fixed as tapering ratio, perforation shape, perforation size and perforation layout. The tapered steel section with perforation has lower critical shear buckling load and efficiency compared to tapered section without perforation but obtains a higher critical shear buckling load and efficiency compared to uniform section without perforation. The smaller the opening size and tapering ratio contributes to a larger of shear buckling capacity and efficiency of the section. The perforation layout with different perforation arrangement and spacing affect the shear strength and efficiency of the tapered steel section with perforation. The highest efficiency model is selected as section with 0.4D diamond perforation in layout 3 under tapering ratio of 0.3. The critical shear buckling load and efficiency is reduced 14.39% and 13.91% respectively when perforations are added onto the tapered steel section. A total of 0.56% steel material can be saved for same structural construction by using tapered steel section with perforation compared with tapered steel section without perforation.

TABLE OF CONTENTS

ACKNOWLEDGEMENT ..... **I**.

ABSTRAK ..... **II**.

ABSTRACT ..... **III.**

TABLE OF CONTENTS ..... **IV**

LIST OF FIGURES ..... **VII**

LIST OF TABLES ..... **XII**.

LIST OF ABBREVIATIONS ..... **XIII**.

LIST OF NOMENCLATURES ..... **XIV**.

CHAPTER 1 ..... **1**.

1.1 General 1

1.2 Tapered steel 2

1.3 Peforation 3

1.4 Structural efficiency 4

1.5 Shear 6

1.6 Problem statement 9

1.7 Objective 9

1.8 Scope of work 10

1.9 Importance and benefits of the research 11

CHAPTER 2 ..... **12**

2.1 Introduction 12

2.2 Perforation shape 13

2.3 Perforation size 18

2.4 Peforation layout 22

2.5 Tapering ratio 25

2.6 Efficiency 29

2.7 Summary 30

CHAPTER 3 31

3.1 Introduction 31

3.2 Finite element analysis by LUSAS software 34

3.2.1 Modelling procedure 35

3.2.2 Model attribute 47

3.2.2.1 Mesh attribute 47

3.2.2.2 Geometric attribute 49

3.2.2.3 Material attribute 49

3.2.2.4 Support and load attribute 50

3.3 Convergebce study 51

3.4 Verification study 54

3.4.1 Displacement verification 55

3.4.2 Sher strength verification 58

3.4.3 Eigenvalue verification 62

CHAPTER 4 64

4.1 Introduction 64

4.2 Finite element models 65

4.3 Results 66

4.3.1 Results of shear buckling deformation pattern 66

4.3.2 Results of shear buckling deformation pattern 80

4.3.2.1 Calculation example 84

4.4 Effect of perforation shape 88

4.5 Effect of perforation size 93

4.6 Effect of perforation layout 98

4.7 Effect of tapering ratio 103

4.8 Model with highest efficiency 108

4.8.1 Comparison in shear deformation pattern 108

4.8.2 Comparison in critical shear buckling load and efficiency 110

CHAPTER 5 113

5.1 Conclusion 113

5.2 Recommendation for Future Research 114

REFERENCES 115

LIST OF FIGURES

Figure 1.1: 3D view of tapered steel beam section. (Azar, 2015) 2

Figure 1.2: Different portal frame configured with tapered members (Marques et al., 2014)..... 3

Figure 1.3: Geometric configurations of web openings (left) and rotated elliptical web openings (right) (Tsavdaridis and Mello, 2012)..... 4

Figure 1.4: General scheme of rotated Stress Field model (Estrada et al., 2006). 6

Figure 1.5: Out of plane deformation shape (Gendy, 2014). 7

Figure 1.6: Illustration for MSM (Studer et al., 2015)..... 8

Figure 2.1: Von-Mises stresses of beams subjected to high shear forces for different type of openings (Tsavdaridis and Mello, 2009). 13

Figure 2.2: Moment shear interaction curves for various web opening (Tsavdaridis and Mello, 2009). 14

Figure 2.3: Contour of buckling mode of (a) TriWP - circle - 0.5; (b) TriWP - square - 0.5; (c) TriWP - diamond - 0.5; (d) TriWP - hexagon - 0.5 (Kong, 2012). 15

Figure 2.4: Result of contour for TriWP with perforation of diamond in shape and 0.4D in size for Mode 1. (Hassan, 2016)..... 16

Figure 2.5: Shear buckling capacity of TriWP with perforation of 0.4D. (Hassan, 2016) 17

Figure 2.6: Four zones of *Vierendeel* mechanism in the opening. (Lagaros et al., 2008)..... 18

Figure 2.7: Contour of buckling mode of (a) TriWP - circle - 0.5; (b) TriWP - circle - 0.4; (c) TriWP - circle - 0.3; (d) TriWP - circle - 0.2; (e) TriWP – circle – 0.1.(Kong, 2012)..... 19

Figure 2.8: Effect of perforation size on maximum deformation of the plate. (Gendy, 2014)..... 21

Figure 2.9: Tensile and compressive stresses of tapered beam subjected to pure shear force. (Gendy, 2014)..... 22

Figure 2.10: The isometric view of TriWP with perforation of circular shaped arranged in (a) Layout 1; (b) Layout 2; (c) Layout 3. (Hasan, 2016) 23

Figure 2.11: Shear Buckling Capacity versus Number of Opening per Meter Length. (Ng, 2017)..... 24

Figure 2.12: Location of maximum stress under a uniform distributed load for section with different tapering ratio under UDL (Kim et al., 2013) 25

Figure 2.13: Location of maximum stress under a uniform distributed load for section with different tapering ratio under point load (Kim et al., 2013)..... 26

Figure 2.14: Graph of critical shear load against tapering ratio of the plate without perforations of different aspect ratio. (Gendy, 2014)..... 27

Figure 2.15(a): Relation of critical shear load ratio and circular diameter to the average depth ratio x=1.0 with α=1.0 (Gendy, 2014) 27

Figure 2.15(b): Relation of critical shear load ratio and circular diameter to the average depth ratio x=1.0 with α=1.2 (Gendy, 2014) 28

Figure 2.15(c): Relation of critical shear load ratio and circular diameter to the average depth ratio x=1.0 with α=1.5 (Gendy, 2014) 28

Figure 3.1: Framework for methodology. 33

Figure 3.2: Modelling procedure by using LUSAS software 35

Figure 3.3: Setting for file details and model details for creating new model 36

Figure 3.4 Location of the point and line button. 37

Figure 3.5: Coordinate table to set origin. 37

Figure 3.6: Sweep table for X, Y and Z direction 38

Figure 3.7: I-beam geometry 39

Figure 3.8: Tapered beam geometry 39

Figure 3.9: Enter coordinate of the circle 40

Figure 3.10: Tapered beam with perforation 40

Figure 3.11: Surface mesh attribute table 41

Figure 3.12: Geometric surface attribute table 42

Figure 3.13: Material library attributes table 42

Figure 3.14: Structural supports attributes table 43

Figure 3.15: Concentrated load attributes table 44

Figure 3.16: Eigenvalue activation steps 45

Figure 3.17: Eigenvalue activation table 45

Figure 3.18: Position of "Solve Now" button 46

Figure 3.19: Regular transition mesh and irregular mesh 47

Figure 3.20: Number of nodes for element TSL6 and QSL8 48

Figure 3.21: Differences between TSL6 and QSL8 48

Figure 3.22: Support and loading condition of model for shear analysis 50

Figure 3.23: Model used in convergence study 51

Figure 3.24: Graph of displacement against element number for convergence study 53

Figure 3.25: Displacement result from LUSAS software 55

Figure 3.26: Models used for shear strength verification 58

Figure 3.27: Model used for eigenvalue verification 62

Figure 4.1: Typical section properties for all models. 63

Figure 4.2: Shear deformation pattern of steel sections with 0.3 tapering ratio, circle perforation and perforation size of (a) 0.4D; (b) 0.5D; (c) 0.6D; (e) 0.7D 67

Figure 4.3: Shear deformation pattern of steel sections with 0.3 tapering ratio, circle perforation and perforation size of (a) 0.4D; (b) 0.5D; (c) 0.6D; (e) 0.7D 68

Figure 4.4: Shear deformation pattern of steel sections with 0.3 tapering ratio, hexagon perforation and perforation size of (a) 0.4D; (b) 0.5D; (c) 0.6D; (e) 0.7D 69

Figure 4.5: Shear deformation pattern of steel sections with 0.3 tapering ratio, square perforation and perforation size of (a) 0.4D; (b) 0.5D; (c) 0.6D; (e) 0.7D 70

Figure 4.6: Shear deformation pattern of steel sections with 0.5 tapering ratio, circle perforation and perforation size of (a) 0.4D; (b) 0.5D; (c) 0.6D; (e) 0.7D 71

Figure 4.7: Shear deformation pattern of steel sections with 0.5 tapering ratio, diamond perforation and perforation size of (a) 0.4D; (b) 0.5D; (c) 0.6D; (e) 0.7D 72

Figure 4.8: Shear deformation pattern of steel sections with 0.5 tapering ratio, hexagon perforation and perforation size of (a) 0.4D; (b) 0.5D; (c) 0.6D; (e) 0.7D. 73

Figure 4.9: Shear deformation pattern of steel sections with 0.5 tapering ratio, square perforation and perforation size of (a) 0.4D; (b) 0.5D; (c) 0.6D; (e) 0.7D. 74

Figure 4.10: Shear deformation pattern of steel sections with 0.7 tapering ratio, circle perforation and perforation size of (a) 0.4D; (b) 0.5D; (c) 0.6D; (e) 0.7D 75

Figure 4.11: Shear deformation pattern of steel sections with 0.7 tapering ratio, diamond perforation and perforation size of (a) 0.4D; (b) 0.5D; (c) 0.6D; (e) 0.7D 76

Figure 4.12: Shear deformation pattern of steel sections with 0.7 tapering ratio, hexagon perforation and perforation size of (a) 0.4D; (b) 0.5D; (c) 0.6D; (e) 0.7D. 77

Figure 4.13: Shear deformation pattern of steel sections with 0.7 tapering ratio, square perforation and perforation size of (a) 0.4D; (b) 0.5D; (c) 0.6D; (e) 0.7D 78

Figure 4.14: Shear deformation pattern of steel sections without perforation with tapering ratio of (a) 0.3; (b) 0.5; (c) 0.7; (e) uniform I beam 79

Figure 4.15: Geometric configuration of different web openings 88

Figure 4.16(a): Typical deformation pattern for circular opening 89

Figure 4.16(b): Typical deformation pattern for hexagon opening 90

Figure 4.16(c): Typical deformation pattern for diamond opening 90

Figure 4.16(d): Typical deformation pattern for square opening 90

Figure 4.17: Graph of efficiency for different types of perforation shape for steel section with tapering ratio of 0.5, perforation size 0.4D in layout 1 92

Figure 4.18: Geometric configuration of different opening sizes 93

Figure 4.19(a): Typical shear deformation pattern for 0.4D opening size 94

Figure 4.19(b): Typical shear deformation pattern for 0.5D opening size 95

Figure 4.19(c): Typical shear deformation pattern for 0.6D opening size 95

Figure 4.19(d): Typical shear deformation pattern for 0.7D opening size 95

Figure 4.20: Graph of efficiency for different perforation size for steel section with diamond opening and tapering ratio of 0.5 in layout 1. 97

Figure 4.21(a): Geometric configuration of layout 1. 98

Figure 4.21(b): Geometric configuration of layout 2. 98

Figure 4.21(c): Geometric configuration of layout 3. 98

Figure 4.22(a): Typical shear deformation pattern of layout 1 100

Figure 4.22(b): Typical shear deformation pattern of layout 2 100

Figure 4.22(c): Typical shear deformation pattern of layout 3 100

Figure 4.23: Graph of efficiency for different perforation layout for steel section with tapering ratio of 0.5 and perforation size of 0.4D for circular opening. 102

Figure 4.24(a): Geometric configuration for tapering ratio of 0.3. 103

Figure 4.24(b): Geometric configuration for tapering ratio of 0.5. 103

Figure 4.24(c): Geometric configuration for tapering ratio of 0.7. 103

Figure 4.25(a): Typical shear deformation pattern for tapering ratio of 0.3 for square opening 105

Figure 4.25(b): Typical shear deformation pattern for tapering ratio of 0.5 for square opening 105

Figure 4.25(c): Typical shear deformation pattern for tapering ratio of 0.7 for square opening 105

Figure 4.26: Graph of efficiency for different tapering ratio for steel section with perforation size of 0.4D, perforation layout 1 for circular opening 107

Figure 4.27: Shear deformation pattern for model with highest efficiency 109

Figure 4.28: Shear deformation pattern for steel section with tapering ratio of 0.3 without perforation. 109

Figure 4.29: Shear deformation pattern for uniform section without perforation 109

Figure 4.30: Graph of efficiency of different section 111

LIST OF TABLES

Table 2.1: The structural efficiency of TriWP with perforation (Hasan, 2016) 29

Table 2.2: Percentage difference of structural efficiency (Hasan, 2016)..... 30

Table 3.1: Element groups of LUSAS (LUSAS Modeller User Manual, 2014) 47

Table 3.2: Section properties of model used in convergence study 52

Table 3.3: Details of models for convergence study..... 53

Table 3.4: Section properties of model used for displacement verification 55

Table 3.5: Section properties of model used for shear strength verification 59

Table 3.6: Comparison of shear strength from theoretical computation and LUSAS software analysis. 61

Table 3.7: Section properties of model for eigenvalue verification..... 62

Table 3.8: Eigenvalue and shear buckling capacity of model for different applied load. 63

Table 4.1: Result for steel sections with 0.3 tapering ratio 81

Table 4.2: Result for steel sections with 0.5 tapering ratio 82

Table 4.3: Result for steel sections with 0.7 tapering ratio 83

Table 4.4: Radius and area for each opening for section with tapering ratio 0.3, circle perforation, 0.4D perforation size in layout 1. 86

Table 4.5: Perforation area and shear buckling load of different perforation shape for steel section with tapering ratio of 0.5, perforation size 0.4D in layout 1 92

Table 4.6: Perforation area and shear buckling load of different perforation size for steel section with diamond opening and tapering ratio of 0.5 in layout 1 97

Table 4.7: Perforation area and shear buckling load of different perforation layouts for steel section with tapering ratio of 0.5, perforation size of 0.4D of circular openings. 102

Table 4.8: Depth of web for different tapering ratio 103

Table 4.9: Perforation area and shear buckling load of different tapering ratio for steel section with perforation size of 0.4D, perforation layout 1 of circular openings. 107

Table 4.10: Critical Shear Buckling Load for different sections. 110

LIST OF ABBREVIATIONS

BSM	Basic Shear Method
FEA	**F**inite **E**lement **A**nalysis
MSM	Modified Shear Method
TriWP	Triangular web profile
COCOC	**C**lose-**O**pen-**C**lose-**O**pen-**C**lose
OCOCO	**O**pen-**C**lose-**O**pen-**C**lose-**O**pen
OOOOO	**O**pen-**O**pen-**O**pen-**O**pen-**O**pen

LIST OF NOMENCLATURES

B	Width of section
D	Depth of section at particular opening location
E	Modulus elasticity
h_{max}	Maximum depth of the section
h_{min}	Minimum depth of the section
I	Moment of inertia
L	Length of the section
P	Applied load
t_f	Flange thickness
t_w	Web thickness
v	Poisson ratio

CHAPTER 1

INTRODUCTION

1.1 General

In this research, the efficiency of tapered steel section with perforation under shear behaviour was studied. Steel is a common construction material with high stiffness, ductility, strength and toughness. I-section beam is a type of joist or girder made from structural steel which is well recognized for the design of long span beams that carry high load and flexural efficiency about the strong axis. Ordinary shape of I-section beam is constructed from two parallel flanges and a flat web. In construction application, most of the compressive stress and transmits shear in the beam are catered by the web while the flanges support the major external loads. In order to reduce the weight and cost of the design without weakening the load carrying capability of the beam, thin webs are required. However, the problem of plate buckling may occur if the web is extremely slender. Possible ways such as using thicker plates, web stiffeners or strengthening the web by making it corrugation have been introduced to solve the slenderness problems but not cost effective. Hence, tapered steel section with perforation is introduced to achieve optimization in construction.

1.2 Tapered steel

Tapered steel section is a section consisting of two flanges connected by tapered web. The use of beams with variable cross-sections has been increasing in the steel construction industry due to the ability in increasing structural stability, satisfying architectural demand in aesthetics, fulfilling functional requirements and reducing weight and cost in many fields. Tapered members are commonly applied in steel frames, namely industrial halls, warehouses, exhibition centres and others. The reduction of self-weight of beams by tapering on web profile can lead to the great saving of column and pile cap materials as well for a lighter dead load. In the design of cantilever steel beam structures, tapering is introduced at the web profile to achieve utmost economy and suit the bending moment distributions. The varying of cross section of web allows a more uniform stress is obtained along the members. The tapering ratio is defined as ratio between the maximum and the minimum height of the tapered member.

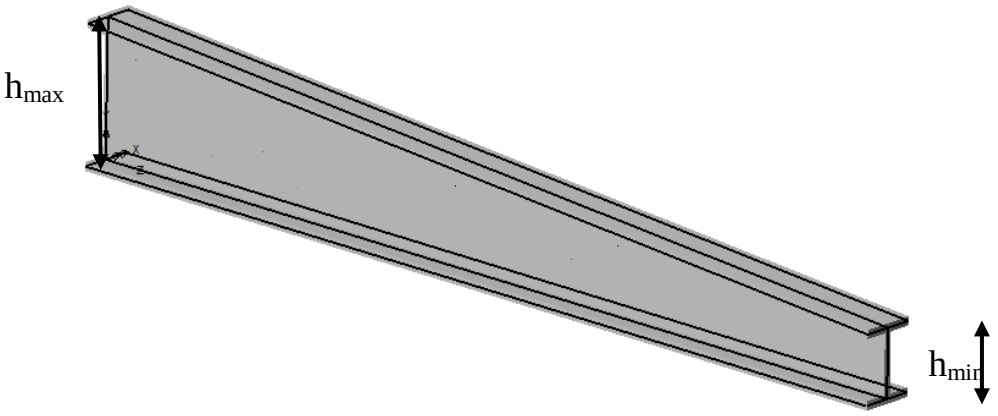

Figure 1.1: 3D view of tapered steel beam section. (Azar, 2015)

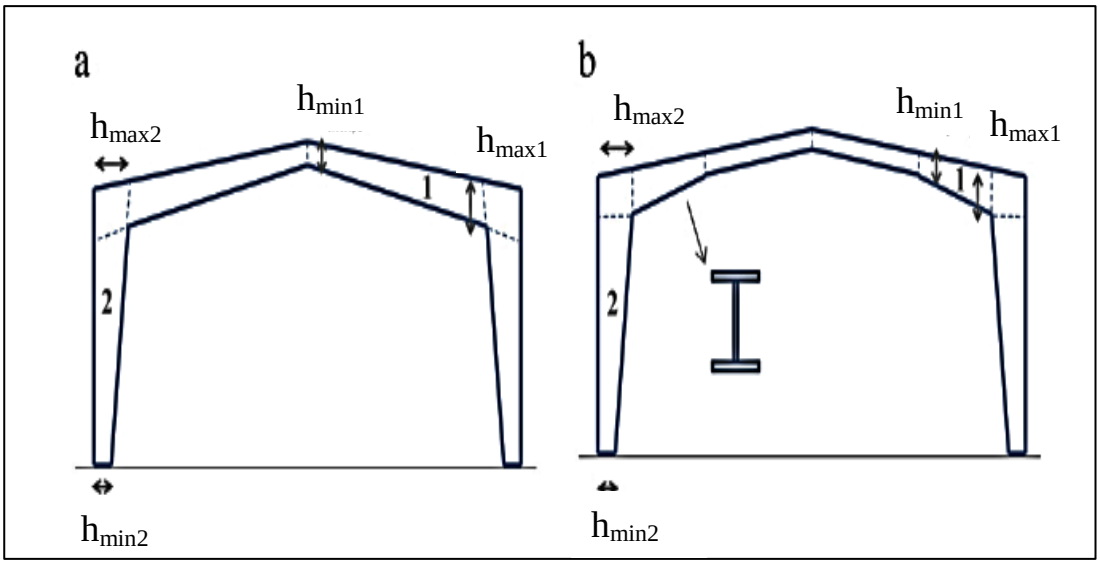

Figure 1.2: Different portal frame configured with tapered members (Marques et al., 2014).

1.3 Perforation

Web profile with openings for steel beams is introduced to reduce the material volume without affecting the structural strength or serviceability requirements. Besides, perforation on web beam is designed to incorporate services within the floor–ceiling zone of the structure. Furthermore, it benefits in alleviating the beam–column joints from high stresses and has a significant effect on the stress distribution and deformation characteristics. Lagaros et al., (2008) stated that the provision of multiple openings in the beams has also been adopted for architectural considerations. Liu and Chung, (2003) mentioned that there are various of perforation shape available such as circle, square, diamond and hexagon. The size of openings also varies from 0.2D to 0.8D. The shapes, sizes and the locations of the opening will affect the performance of beams with given loading and support conditions.

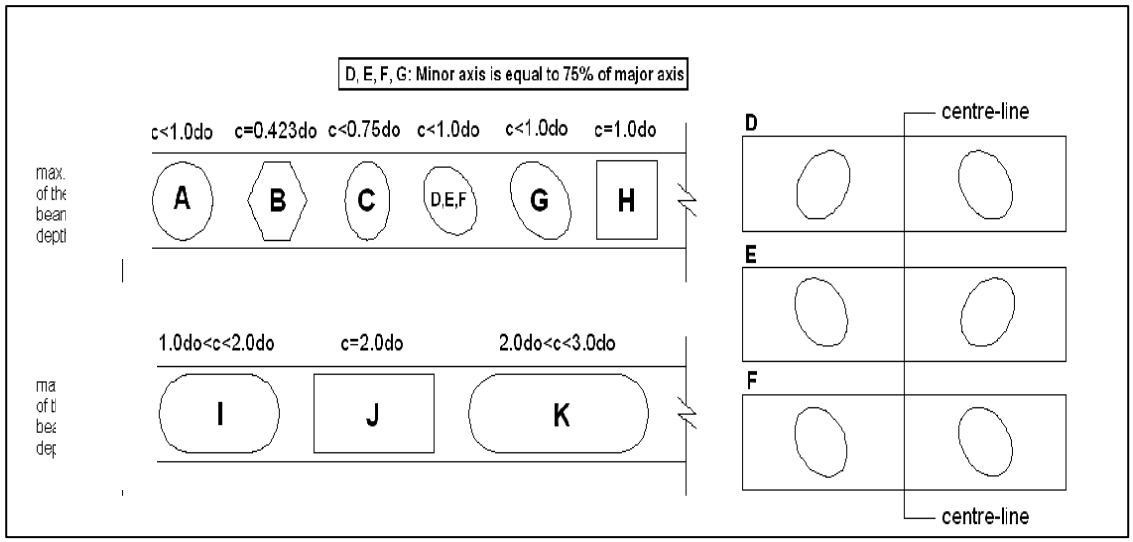

Figure 1.3: Geometric configurations of web openings (left) and rotated elliptical web openings (right) (Tsavdaridis and Mello, 2012).

1.4 Structural efficiency

Efficiency of a structure is measured in terms of weight of material provided to carry a given amount of load. The efficiency of an element is regarded as high if the ratio of its strength to its weight is high. Macdonald (2001) mentioned that the shapes of structural elements especially for the longitudinal axis in relation to the applied load have a great influence on the types and magnitude of the internal force within them. In other words, the efficiency of the structural element is influenced by two main factors including size of the span and its external load-carrying capacity. Hasan (2016) stated that maximum economy can be achieved by controlling the level of complexity of the structure with reasonable efficiency level.

For a particular cross-sectional shape, the structural efficiency of a beam decreases as the length of the span increases. Hasan (2016) concluded that in order to achieve a high efficiency of a structure, the self-weight of the structure is reduced as much as possible without compromising the load carrying capacity of the steel section. Tapering and perforating on the web profile are the effective ways in reducing self-weight. Hence, the efficiency of the section is dependent on the variables of tapering ratio, perforation shape, perforation size and perforation layout. Equation 1.1 and 1.2 show the calculation of self-weight and efficiency of a structure. The critical shear buckling load obtained from the non-linear eigenvalue analysis is used to calculate efficiency of tapered steel section with perforation under shear behaviour.

Eq. (1.1)

$$self - weight\ of\ perforated\ section$$

$$= \frac{self - weight\ of\ section\ without\ perforation}{perforations\ number\ x\ self - weight\ of\ each\ perforations.}$$

$$Efficiency = \frac{Load\ applied}{self - weight\ of\ perforated\ section}$$ Eq. (1.2)

1.5 Shear

Shear is a strain produced by pressure in the structure when its layers are laterally shifted in relation to each other. For stainless steel plate girder, a new design expressions based on Rotated Stress model is invented by Estrada et al., (2006) to predict the ultimate shear strength.

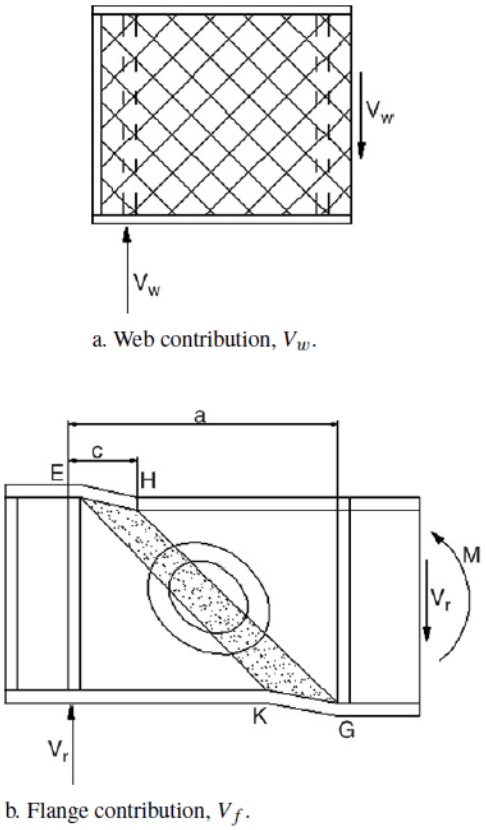

a. Web contribution, V_w.

b. Flange contribution, V_f.

Figure 1.4: General scheme of rotated Stress Field model (Estrada et al., 2006)

Gendy (2014) explained that the diagonal shear buckling is due to the compression caused waves. The number of waves increases when the aspect ratio increases as shown in Figure 1.5. For small aspect ratio, only one wave occurs due to compression diagonal. For large aspect ratio, more than one wave will occur with different amplitudes.

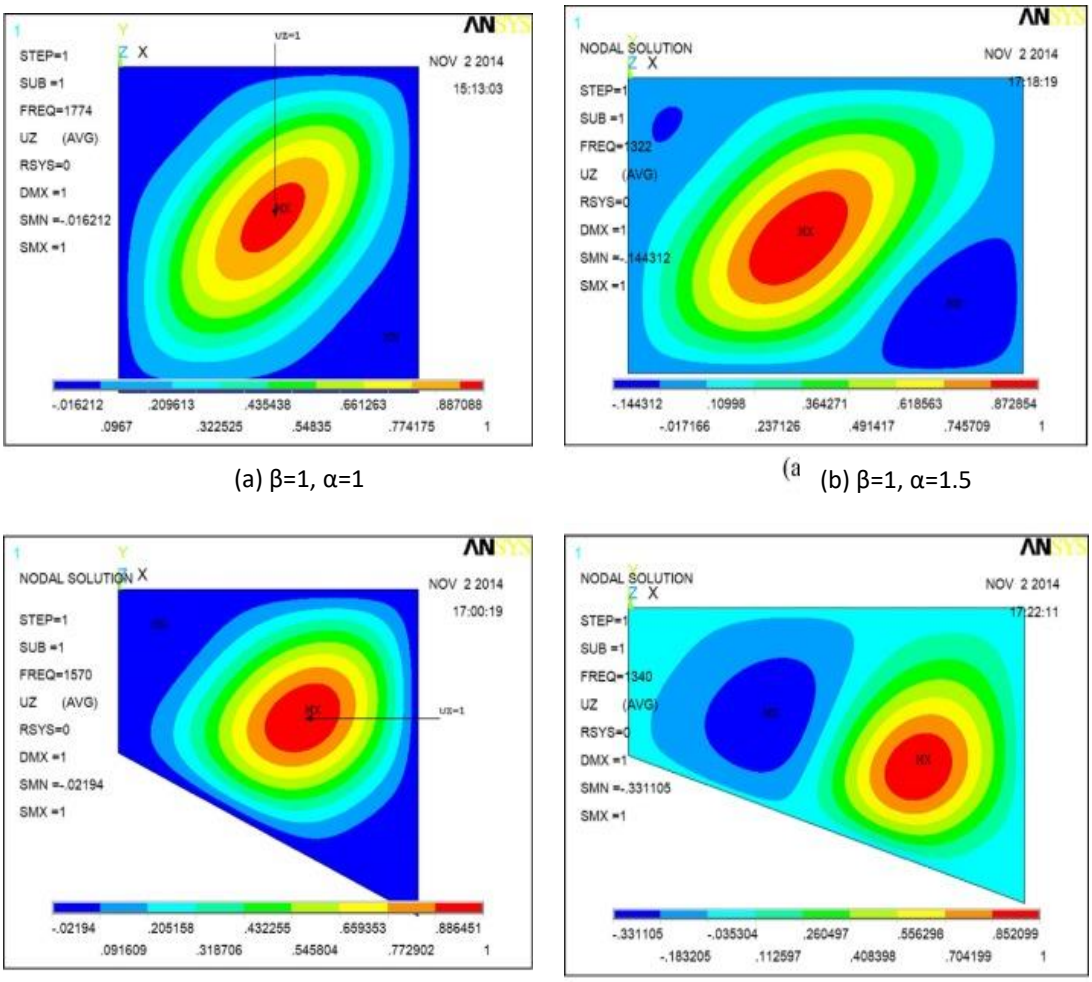

(a) β=1, α=1 (b) β=1, α=1.5

(c) β=0.5, α=1 (c) β=0.5, α=1.5

Figure 1.5: Out of plane deformation shape (Gendy, 2014)

For a plate girder with practical span, the induced shear force in the web is relatively low compared with axial force in the flanges. The thickness of web plate is generally smaller than the flanges. When there is high shear force acting on a conventional I beam, the web of the beam loses its stability and deforms transversely. Serror (2011) stated that the shear capacity is well estimated for prismatic web panels in most of the design codes. However, the shear capacity for tapered web panels are lacking investigation.

Basically, tapered girder web shear can be determined using the Basic Shear Method (BSM) which assigns all shear to the web or Modified Shear Method (MSM) which includes the effect of flange force vertical components that may decrease or increase the web shear force. Figure 1.6 shows the illustration of MSM by Studer et al., (2015). However, both methods are only suitable for tapered steel section without perforation. Hence finite element software is required in this research to determine the shear buckling load and shear deformation of the tapered steel section with perforation.

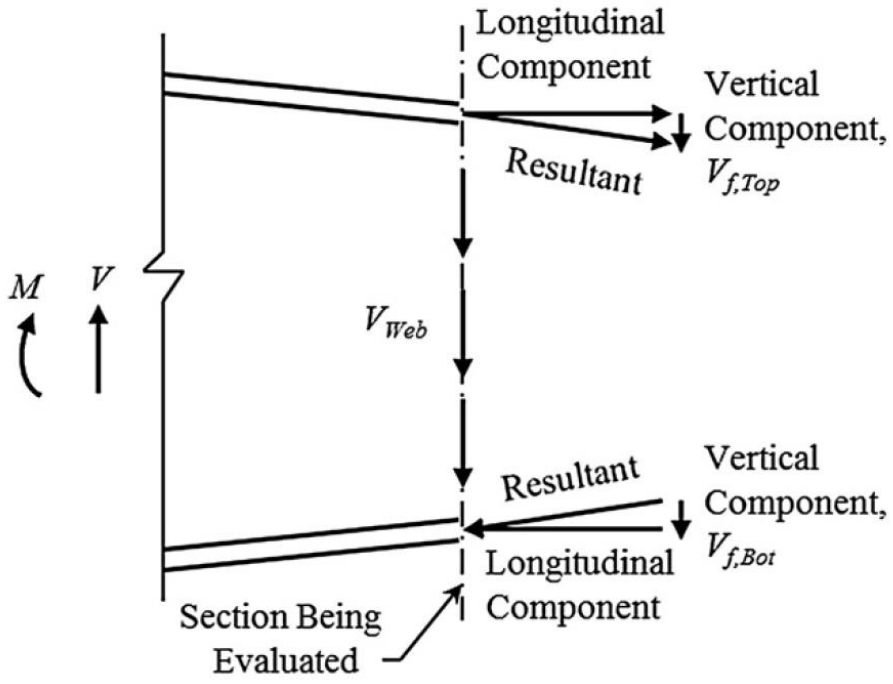

Figure 1.6: Illustration for MSM (Studer et al., 2015).

1.6 Problem statement

The introduction of tapered steel with perforation has reduced the cost and material effectively in construction. Nevertheless, web panel with perforation is prone to deform with combination acting of shear and bending. The stress distribution is not uniform when the section is tapered.

In order to overcome these problems for tapered steel section with perforation, investigation on the efficiency and shear behaviour is needed to assure the design of tapered steel section with perforation is safe and achieve similar performance as the section without opening.

There are different researches on the shear strength of the tapered steel section with perforation. However, there is a research gap of studying efficiency of tapered steel section with perforation under shear behaviour. The tapered-perforated steel section with optimum shear strength may not necessary achieved the highest efficiency. Hence, investigation on efficiency of tapered steel section with perforation under shear behaviour is required to assure the optimization in construction.

1.7 Objectives

The first objective for this investigation is to determine the effect of variable parameters on shear resistance and shear deformation pattern of tapered steel section with perforation. The second objective is to determine the effect of variable parameters on efficiency of tapered steel section with perforation.

1.8 Scope of work

This investigation involves several scopes of works. The major work for this investigation is to simulate the tapered steel section with perforations for shear and efficiency analysis. The model simulation is performed by using LUSAS software with the variation of tapering ratio, perforation size, perforation shape and perforation layout. Tapering ratios are set as 0.3, 0.5 and 0.7. Perforation sizes are limited from 0.4D to 0.7D. Perforation shapes available for this investigation are circle, square, diamond, and hexagon. Perforation layouts varies from perforation number of 5 to 3 and followed by 2 for layout 1, layout 2 and layout 3 respectively. The constant parameters are set as 3.5m for length of section, 9mm for thickness of web and 13mm for thickness of flange. The maximum depth of web is controlled as 500mm.

Shear analysis is carried out by running the LUSAS software to obtain eigenvalue for critical shear buckling load. Efficiency analysis is conducted by determining the ratio of critical shear buckling load to the self-weight of the tapered steel sections with perforations. Determination of the model with highest efficiency is essential to compare the shear strength and efficiency with the control models of uniform I-beam and tapered steel section without perforations.

1.9 Importance and benefits of the research

This investigation gives some benefits for steel construction industry. This investigation is important as it will prove the introduction of tapering and perforations on beam enables the saving of steel material in construction field and achieves similar performance as the section without tapering and perforation. When tapering and perforations are applied onto the web of the beam, the steel weight required for the structure is reduced. Hence, this investigation will prove the reduction of cost for steel structures and at the same time improve the steel flexibility and installation with the increasing strength-to-weight ratio of the steel. The shear capacity for tapered web panels with perforations is lack of investigation, therefore this investigation is essential to enhance the safety issue in design of tapered steel section with perforations.

CHAPTER 2

LITERATURE REVIEW

2.1 Introduction

Steel is a common construction material with high strength, stiffness and ductility to resist deformations and stresses. The demand on steel is high especially for tall building, factory, bridges, and stadium. Cost is the controlling element for construction project. The steel price is calculated according to its weight, the higher the steel weight required for the structure, the higher the material cost for the project. The steel price increases dramatically in recent year due to the reason of cutdown production from China. Hence, optimisation in construction is required by reducing construction material. Perforation and tapering are introduced on I-beam to reduce the cost of steel structures. Shear resistance is mostly catered by web of the beam. When web section is reduced by introducing tapering and perforation, the structural strength of the web may be varied. Many researches have been made to investigate separated and integrated effect of tapering and perforation on steel structures to ensure the safety of the design.

2.2 Perforation shape

A finite element investigation of perforated sections with standard and non-standard web opening configurations and sizes was carried out by Tsavdaridis and Mello (2009). The behaviour of the perforated beam with different shape configurations and sizes of web openings were investigated as shown in Figure 2.1. The finding from this research showed that the shear and flexural failures of standard perforation sections are controlled mainly by the web openings size. The critical length of the web openings affects the *Vierendeel* mechanisms. For non-standard web perforations, the structural strength is not only affected by opening depth and critical length of the perforations, but it is strongly influenced by the perforation shape. There are different hinge positions formed for different perforation shapes which contribute to the failure of the beam section UB 457 x 152 x 52, with web openings of depth equal to 0.8h and at a distance, x, of 0.284m from support.

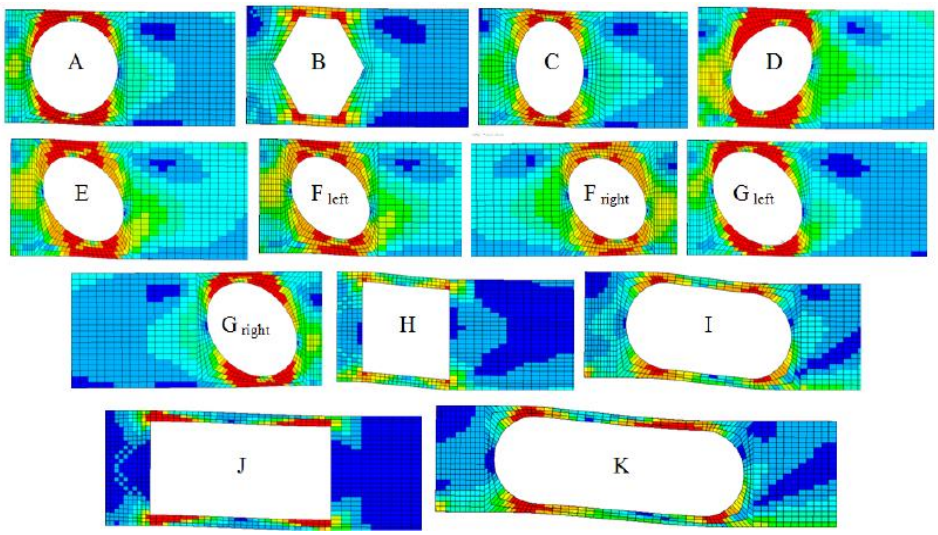

Figure 2.1: Von-Mises stresses of beams subjected to high shear forces for different type of openings. (Tsavdaridis and Mello, 2009).

Figure 2.2 shows the moment shear interaction curves obtained from the finite element investigation. Tsavdaridis and Mello (2009) mentioned that the opening in the web reduced the shear area of the section significantly whilst the reduction of the bending modulus is small. In short, perforated sections with vertical and rotated elliptical web openings have a better performance compared to circular and hexagonal web openings due to the uneven stress distribution.

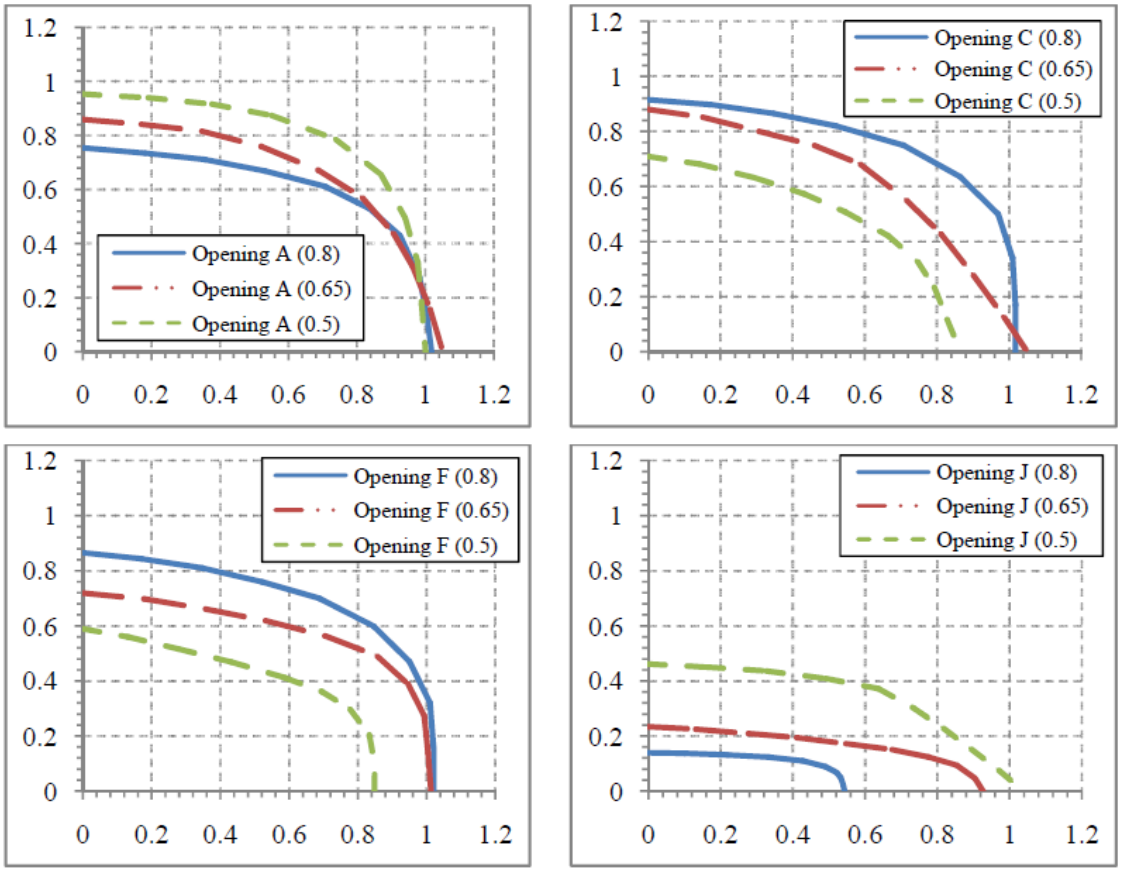

Figure 2.2: Moment shear interaction curves for various web opening (Tsavdaridis and Mello, 2009).

A numerical study on shear behaviour for triangular web profile steel section with openings was completed by Kong (2012). The contours of the buckling mode from the eigenvalue buckling analysis which occurred in the web of triangular web profile with 0.5D opening size is shown as Figure 2.3. The result is summarised that the shear buckling modes for different opening shapes are similar and the shear buckling is significantly around the opening.

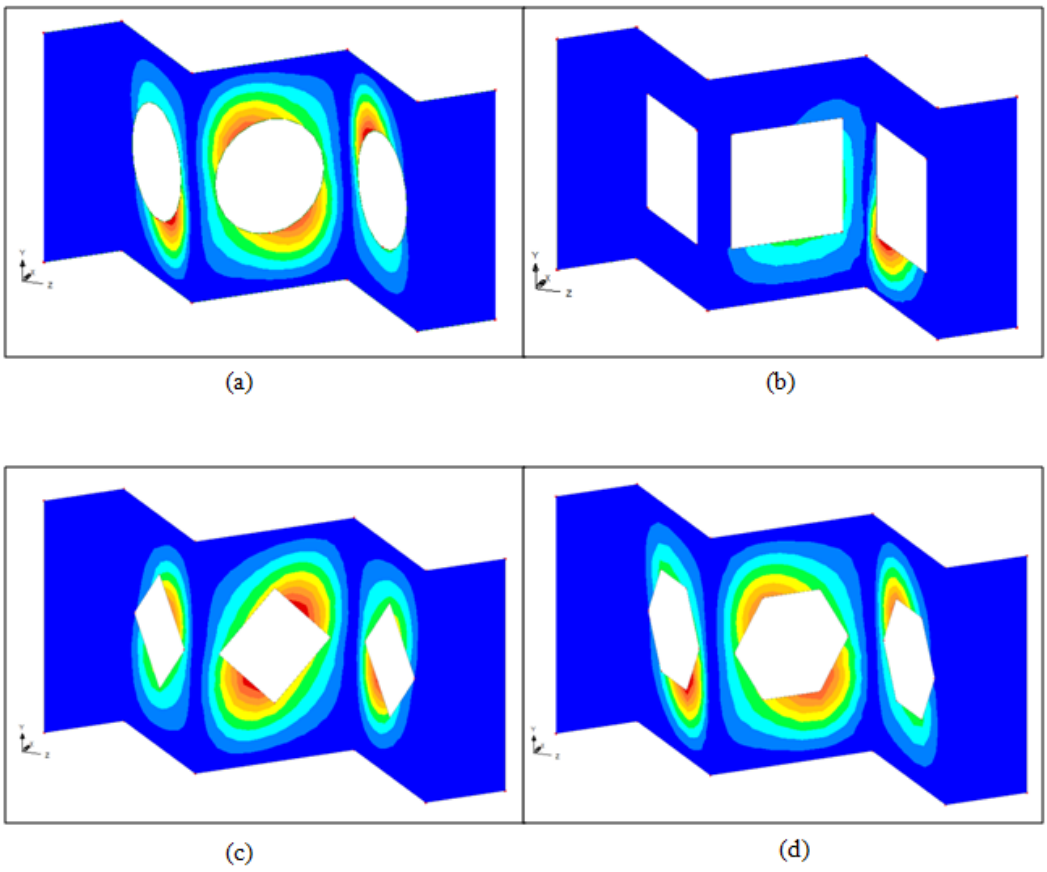

Figure 2.3: Contour of buckling mode of (a) TriWP - circle - 0.5; (b) TriWP - square - 0.5; (c) TriWP - diamond - 0.5; (d) TriWP - hexagon - 0.5 (Kong, 2012).

Hasan (2016) has conducted a study on the efficiency of structural steel section with perforated-corrugated web profile. Figure 2.4 and Figure 2.5 show the shear deformation pattern and shear buckling capacity for different perforation shape on corrugated web profile.

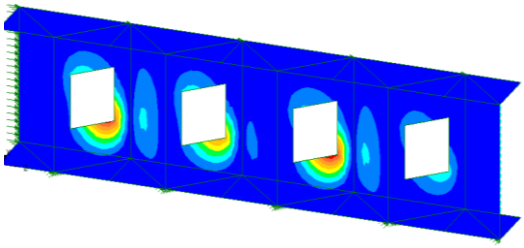

TriWP with square perforation

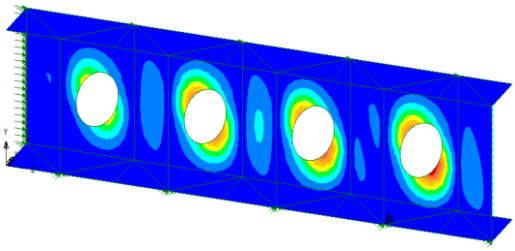

TriWP with circular perforation

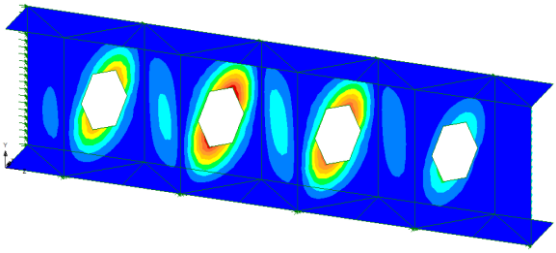

TriWP with hexagonal perforation

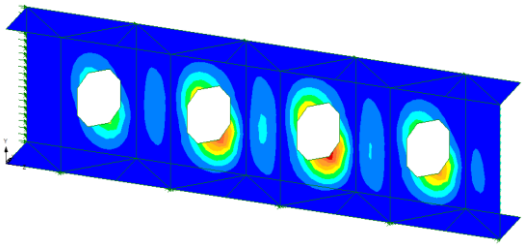

TriWP with octagonal perforation

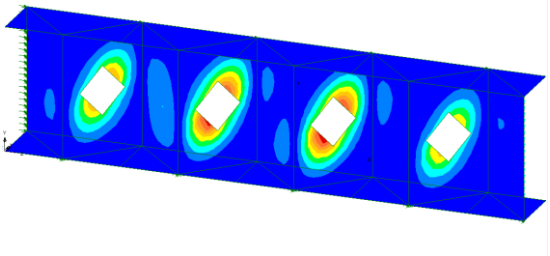

TriWP with diamond perforation

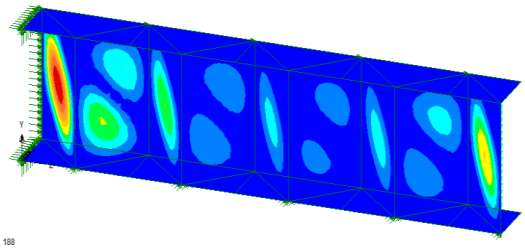

TriWP without perforation

Figure 2.4 Result of contour for TriWP with perforation of diamond in shape and 0.4D in size for Mode 1. (Hassan, 2016)

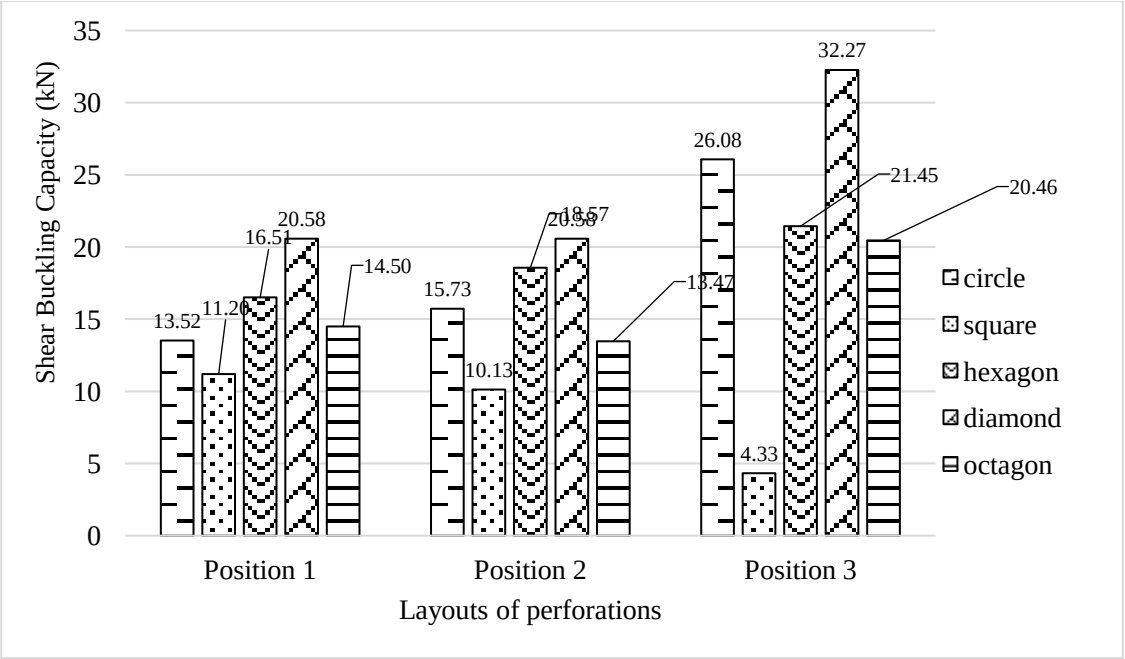

Figure 2.5 Shear buckling capacity of TriWP with perforation of 0.4D. (Hassan, 2016)

Hasan (2016) concludes that perforation of diamond shaped shows the highest shear buckling capacity for Layout 1, Layout 2 and Layout 3 for all three different perforation sizes. On the other hand, square perforation shows the lowest buckling moment resistance for all perforation sizes and layouts. The geometry of a square shape has bigger perforation area compared to other shapes which affects the buckling moment resistance.

2.3 Perforation size

Lagaros et al., (2008) conducted research on optimum design of steel structures with web openings on 3D steel structures. Perforation sizing, shape and topology are the common factors affecting optimization design. The test result showed that the maximum diameter of the circular opening should not be extremely large. The increasing of opening height leads to reduction of both shear and moment capacities, hence the perforated beam is prone to present shear or flexural failure. Furthermore, the possibility for the occurrence of *Vierendeel* mechanism with the characteristic of forming four plastic areas at the corners of the opening is higher for large opening size especially when shear force is high as shown in Figure 2.6.

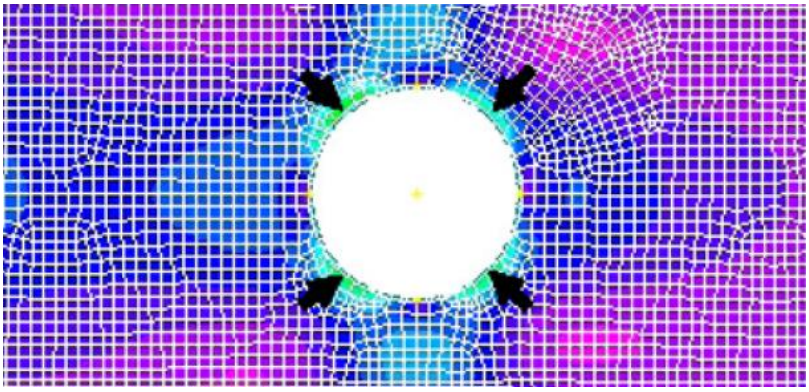

Figure 2.6: Four zones of *Vierendeel* mechanism in the opening. (Lagaros et al., 2008)

Effects of circular or square web openings on the ultimate strength of horizontally curved composite plate girders was conducted by Basher et al., (2009). From the result, it showed that the shear capacity drops steadily as the size of the openings increase. The rate of decrease in shear strength are different for each perforation size where 11% reduction when the opening size is increased from 0.3D to 0.4D, and 5% reduction when the opening size is increased further to 0.5D. It also summarised that the reduction of

ultimate shear strength is small for small opening size and can be neglected, but for perforation with depth exceeding 0.2 times the girder depth, the effects are magnified to an extent that cannot be neglected.

From the numerical study on shear behaviour for triangular web profile steel section with openings by Kong, (2012), it concluded that the contours of shear buckling mode throughout the decrease of opening size are very similar. Figure 2.7 shows the contours of the buckling mode from the eigenvalue buckling analysis which occurred in the web of triangular web profile with circle opening of different opening.

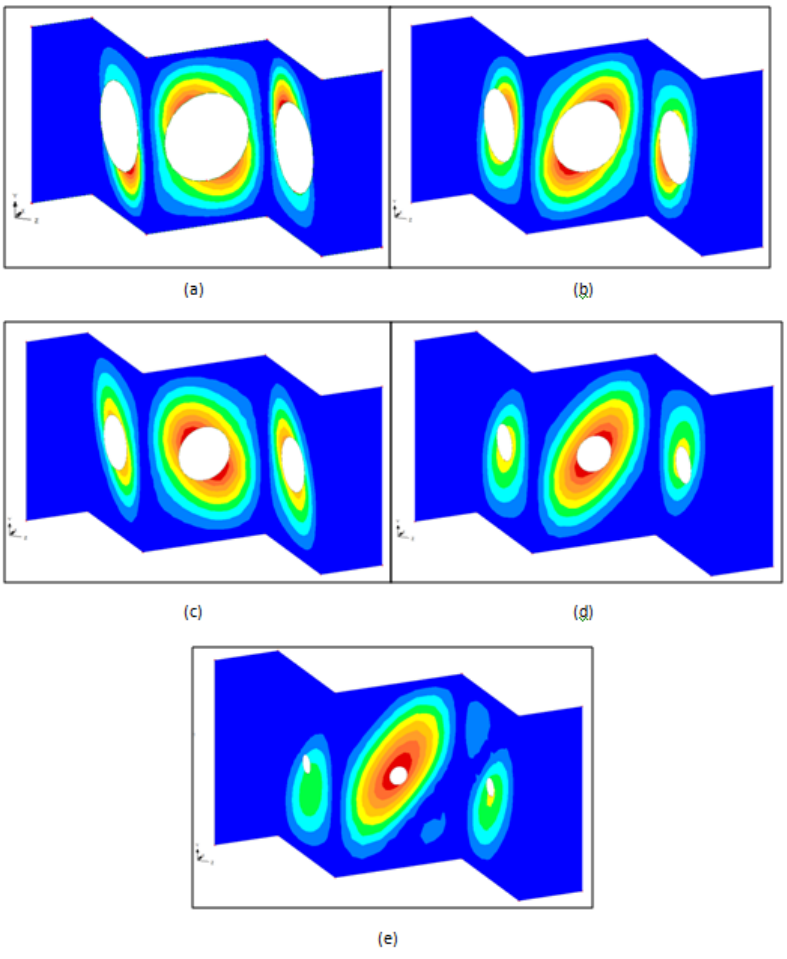

Figure 2.7: Contour of buckling mode of (a) TriWP - circle - 0.5; (b) TriWP - circle - 0.4; (c) TriWP - circle - 0.3; (d) TriWP - circle - 0.2; (e) TriWP – circle – 0.1. (Kong, 2012)

Gendy (2014) analysed the critical shear buckling load of tapered plate with circular opening. From the results, it concludesd that the critical shear load ratio is constant for small opening. For large opening, the critical shear load ratio decreases with the increase in the opening diameter due to lack of plate cross section. Gendy (2014) also found that the maximum out-of-plane deformations occurs at the upper left corner for solid tapered plate and tapered plate will small perforations. The maximum deformations move to the perimeter of the circular opening which is the weaker part of the plate when the perforation size increases as shown in Figure 2.8.

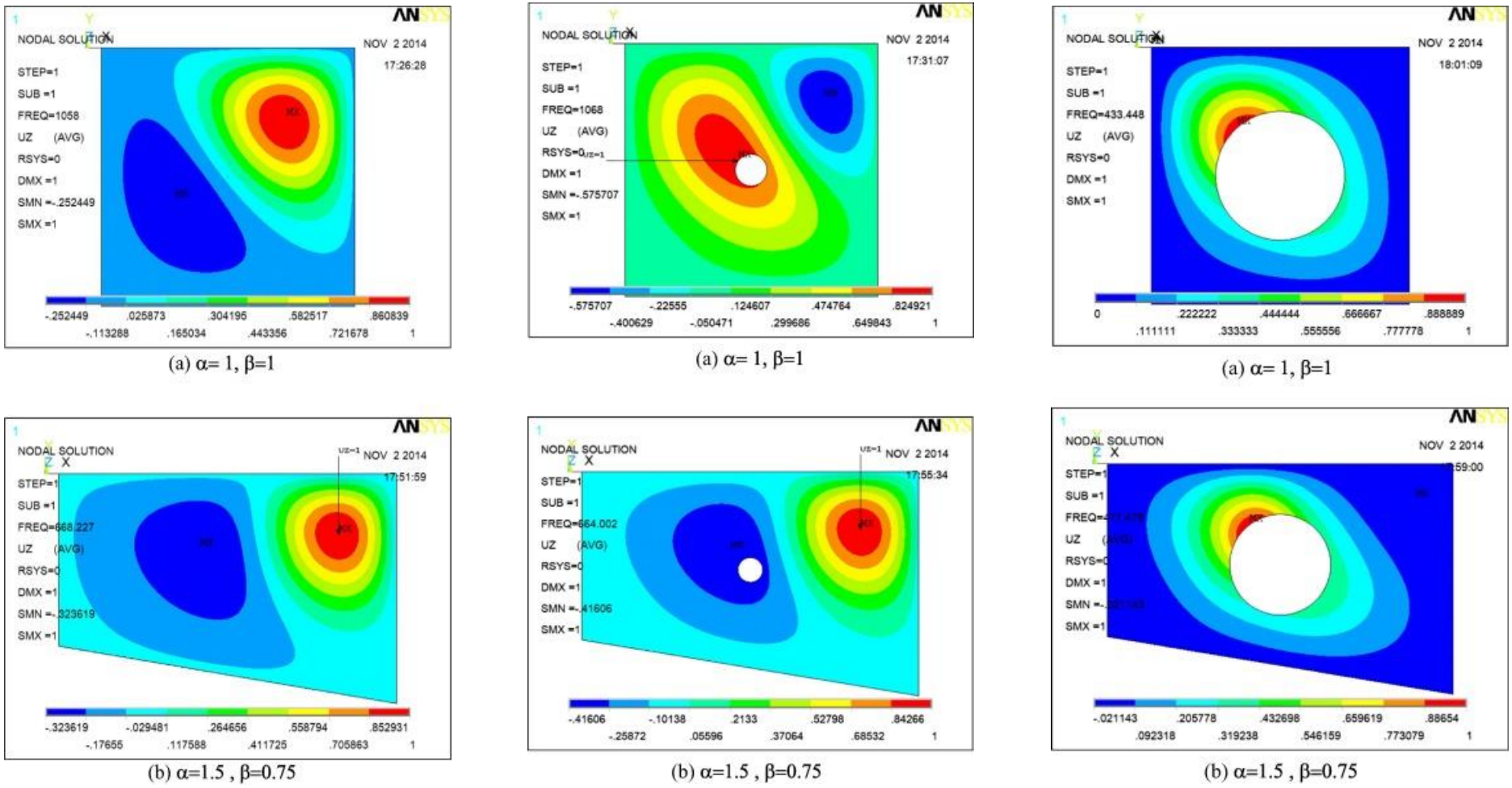

Figure 2.8: Effect of perforation size on maximum deformation of the plate. (Gendy, 2014)

2.4 Perforation layout

Gendy (2014) mentioned that the locations of the openings have great effect on the critical shear load especially when the opening is located at the compression zone as shown in Figure 2.9. The perforation layout will influence the openings' location.

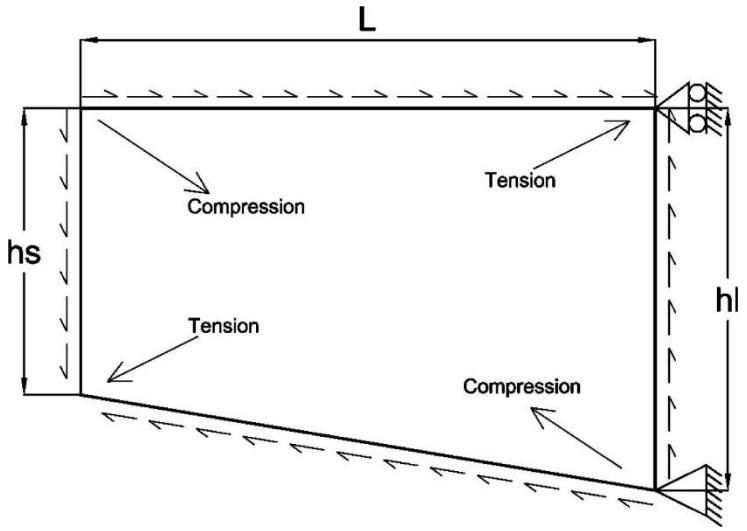

Figure 2.9: Tensile and compressive stresses of tapered beam subjected to pure shear force. (Gendy, 2014)

Hasan (2016) has conducted a research on efficiency of structural steel with different perforation layout on corrugated web profile. The first layout located the perforations along the corrugated web and began form the web near the both ends of the triangular web profile. For layout 2 and layout 3, the perforations located in an alternative arrangement as shown in Figure 2.10. The findings from this research showed that the perforations are arranged in Layout 3 obtains the highest shear buckling capacity due to the reason that the number of perforations in the web section is less than those in Layout 1 and Layout 2.

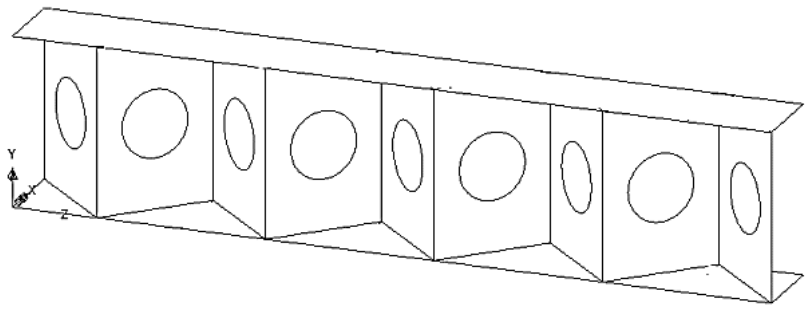

(a)

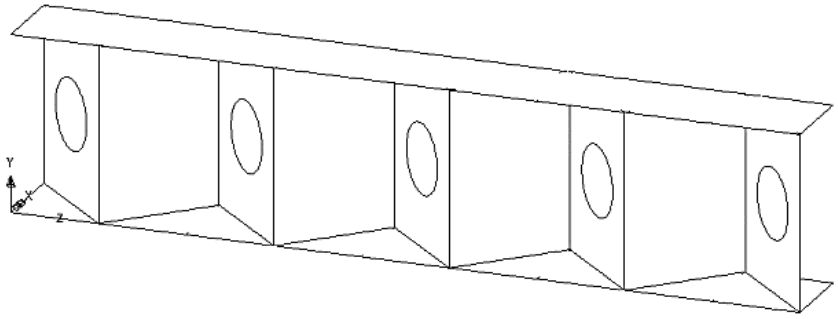

(b)

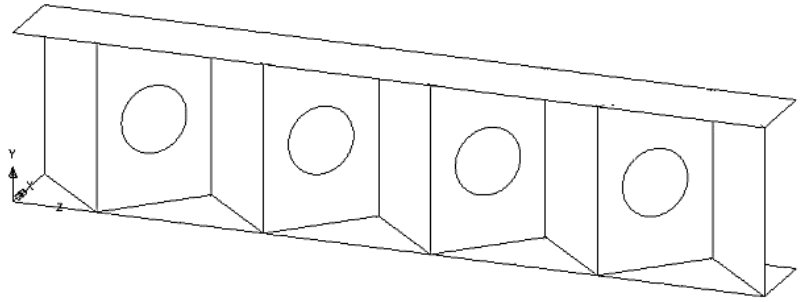

(c)

Figure 2.10: The isometric view of TriWP with perforation of circular shaped arranged in (a) Layout 1; (b) Layout 2; (c) Layout 3. (Hasan, 2016)

Perforation layout is influencing the opening centre to centre distance and the perforation number. Ng (2017) has carried out a numerical study on shear buckling capacity of Z-section steel purlin with opening. From the results, it showed that the shear buckling capacities for opening centre to centre distance of 100mm, 150mm, 200mm and 250mm are 2.45kN, 2.84 kN, 2.82 kN and 2.89kN respectively. For a constant length of section, the number of perforation increases as the opening centre to centre distance decreases. Thus, the shear buckling capacity is larger for layout with smaller perforation number and larger opening centre to centre distance as shown in Figure 2.11.

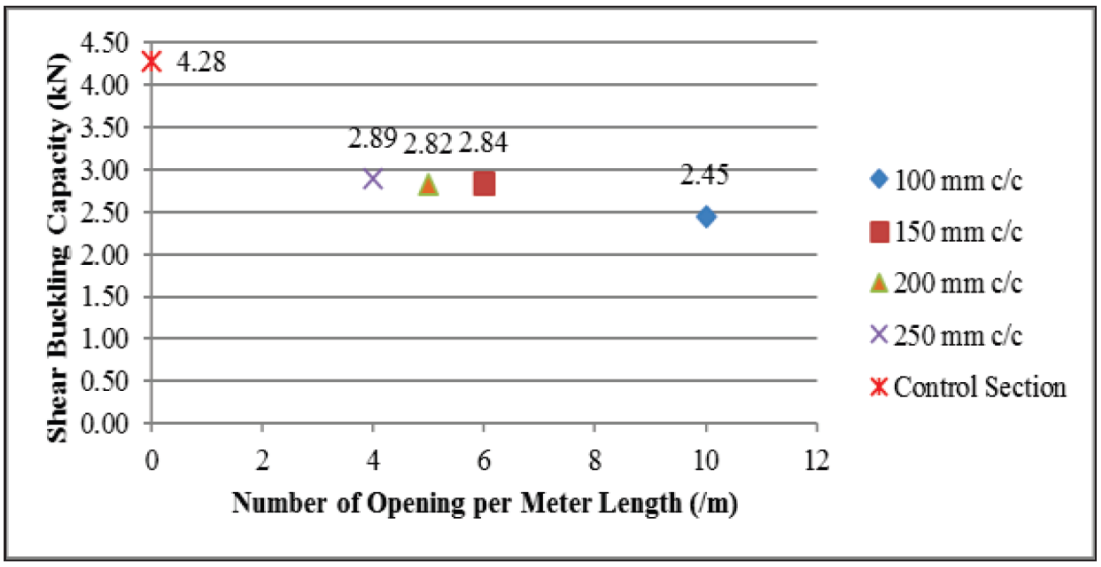

Figure 2.11: Shear Buckling Capacity versus Number of Opening per Meter Length. (Ng, 2017)